Microwave properties of nanodiamond particles

Daniel Slocombe, Adrian Porch, Etienne Bustarret, and Oliver A. Williams
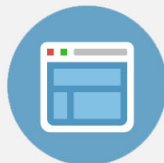
Microwave properties of nanodiamond particles

Daniel Slocombe,[1,2] Adrian Porch,[1] Etienne Bustarret,[3] and Oliver A. Williams[4]

[1]*School of Engineering, Cardiff University, Queen's Buildings, The Parade, Cardiff CF24 3AA, United Kingdom*
[2]*Inorganic Chemistry Laboratory, University of Oxford, South Parks Road, Oxford OX1 3QR, United Kingdom*
[3]*Institut Néel, CNRS & Université Joseph Fourier, 25 rue des Martyrs BP 166, 38042 Grenoble cedex 9, France*
[4]*School of Physics and Astrophysics, Cardiff University, Queen's Buildings, The Parade, Cardiff CF24 3AA, United Kingdom*

The dielectric properties of nanodiamond powders were characterised at microwave frequencies using a cavity perturbation technique, and results were compared with UV Raman spectroscopy. Surface sp^2 hybridisation in the nanodiamond samples was varied by subsequent oxygenation and hydrogenation. Dielectric polarisation and loss increased as the sp^2 hybridisation was increased. The sensitivity to surface bound sp^2 carbon obtained by the microwave cavity technique far exceeds that of comparable techniques (such as Raman spectroscopy) and is much more convenient in practice, lending itself to studies of real-time modification of such powders by external influences (such as temperature and chemical functionalisation). © 2013 AIP Publishing LLC.
[http://dx.doi.org/10.1063/1.4809823]

Nanodiamond particles have recently generated substantial interest in areas as diverse as diamond nucleation, bio-markers, lubrication, and drug delivery.[1–4] The dielectric properties of nanodiamond particles have been sparsely studied due to the difficulty of contact electrode approaches as well as percolation issues when measuring nanoparticles.[5,6] Of particular interest is the degree of sp^2 hybridisation of the resulting C-C bonds versus the sp^3 hybridisation expected in the interior of bulk diamond. In this work, a microwave cavity perturbation technique is proposed to measure the effective relative permittivity of treated nanodiamond powders, which does not require direct electrical contacts to be made to the particles.

Commercial detonation nanodiamond powders were sourced from PlasmaChem GmbH (G01 grade). This material is purified from the detonation product by the supplier with multiple acid treatments. The core particle size is approximately 5 nm. Three nanodiamond samples were made from this material. First, untreated powders were measured, designated U in what follows. Samples were then oxidised by burning the powders in air (designated O), as has been demonstrated by Osswald *et al.*[7] and Hees *et al.*[8] Finally, samples were hydrogenated (designated H) by annealing in hydrogen gas at 10 mbar, 400 °C.[9] Both O and H samples were measured in the microwave cavity. As a comparison, the same volume of carbon black powder (sourced from Alfa Aesar and designated as CB) was also measured.

Micro-Raman spectra were measured in air with a liquid nitrogen cooled UV enhanced CCD detector in the backscattering parallel geometry. A small amount of diamond powder was placed under a ×40 UV objective using the 325 nm line of a HeCd CW laser. The incident power was reduced to the point where there was no drift in the spectral signatures over various acquisition times (typ. 1–20 min). This clearly limited the signal to noise ratio below the value where surface species such as CH_x could be detected at higher Stokes shifts.[10] The spectra of all of the particles as seen in Fig. 1 were very similar, exhibiting clear peaks at 1332 cm^{-1}, characteristic of sp^3 bonding. This peak is broadened by the small size of the crystallites as well as convoluted with the D-band. A strong G-band is evident at higher wavenumbers due to sp^2 bonding, as is a shoulder below the 1332 cm^{-1} peak due to transpolyacetylene at the grain surfaces.[11] It is clear that there is progressively lower intensity of these sp^2 signatures (shoulder below 1332 cm^{-1} and G-band) between the untreated, hydrogen annealed, and air annealed samples respectively. This difference is, however, subtle due to the insensitivity of UV Raman spectroscopy to small surface concentrations of sp^2.[10] Attempts at using larger wavelengths (up to 633 nm) in Raman spectroscopy were unable to distinguish between the different samples.

All microwave measurements are performed in a cylindrical host cavity, shown schematically in Fig. 2. Powdered samples are placed in thin-walled quartz tubes and are
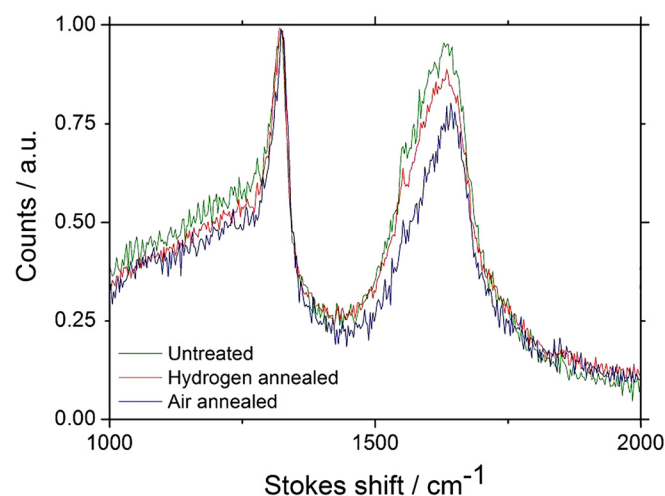

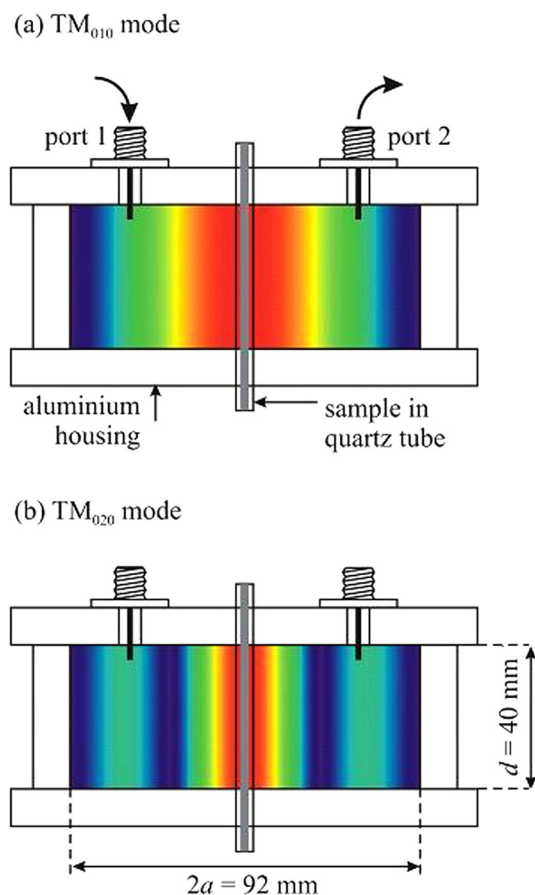FIG. 1. Raman spectra of the three different diamond particle types.

(a) TM_{010} mode

(b) TM_{020} mode

FIG. 2. Schematic diagram of the aluminium host cavity, also showing the magnitude of the electric field in (a) the TM_{010} mode, and (b) the TM_{020} mode. In both cases, the field is parallel to the axis of the cylinder. Samples are introduced along the axis, contained in a thin-walled quartz capillary of inner diameter 2 mm. For such small capillaries, we may assume that the applied field is uniform for both modes.

introduced along the axis of the cavity via small holes drilled in the top and bottom plates. The cavity is machined in three parts from bulk aluminium (for high quality factor Q), with top and bottom plates attached firmly to the cylindrical section using M10 bolts, thus, ensuring good electrical connection at the joints thus formed. The internal dimensions of the cavity are radius $a = 4.6$ cm and length $d = 4.0$ cm, as indicated in Fig. 2.

The TM_{010} and TM_{020} modes are chosen for dielectric property measurement of the samples owing to the high, uniform electric field near the cavity axis.[12] The electric field in these modes is directed parallel to the axis, thus, parallel to the axis of the sample tube, resulting in only minor modifications of the local electric field in the presence of the quartz tube. The distribution of electric field magnitude for each mode is also shown in Fig. 2. For tubes of inner radii $r \ll a$, we may assume the applied electric field to be uniform for each mode. Here, $r/a = 0.022$ so the uniform field approximation is a good one. The radius a is chosen so that the TM_{010} mode has a resonant frequency of about 2.5 GHz. The cavity aspect ratio d/a is chosen to be small enough for the TM_{010} mode to be the dominant mode (i.e., for it to be well below the resonant frequency of the TE_{111} mode), but not too small to significantly compromise the high Q factor or the axial uniformity of the electric field.

Cavity excitation is provided by a pair of square-flanged SMA jack connectors (supplied by Farnell Ltd.), at radial positions 3 cm from the axis. These have open circuit terminations, with an extended center conductor providing capacitive coupling to the electric field of the TM cavity modes. All microwave measurements are performed using an Agilent E5071B network analyser, controlled using LABVIEW software (National Instruments Ltd.). Measurements are performed of the transmitted microwave power $|S_{21}|^2$ in the frequency domain, and non-linear, least-squares curve fitting to a Lorentzian response is used to determine resonant frequencies and loaded quality factors (denoted as Q_L). We remove the effects of cavity couplings by converting Q_L into the unloaded quality factor Q in each case. The cavity couplings are adjusted so that they are equal (i.e., symmetric) and so the conversion is made using the simple formula $Q = Q_L(1 - 10^{-IL/20})$, where IL is the insertion loss (i.e., transmitted power) at resonance, measured in dB.[13] Furthermore, the couplings are kept weak in all circumstances (with $IL < -30$ dB), meaning that very little systematic error is introduced as a result of this decoupling process.

The theoretical values of the resonant frequencies of the TM_{010} and TM_{020} modes of the empty cavity are calculated using $f_{0n0} = cp_{0n}/2\pi a$, where $p_{01} = 2.405$ and $p_{02} = 5.520$ are the first two zeros of the Bessel function $J_0(x)$, giving values of 2.495 and 5.726 GHz, respectively. The measured values are found to be 2.501 and 5.730 GHz, respectively, in excellent agreement with these theoretical values. The unloaded Q factors are measured to be 10 140 and 14 890 for the TM_{010} and TM_{020} modes, respectively, at an ambient temperature of 25 °C. Assuming a resistivity for aluminium of 2.8 $\mu\Omega$ cm, the corresponding theoretical values of the unloaded Q factors are 12 700 and 19 200, respectively. The measured Q factors are lower than the theoretical values by about 25%–30%, as is typical in metal cavities made by traditional machining methods. This is due to the combined effects of increased surface area due to surface roughness (since the skin depth in Al at 2.50 and 5.73 GHz is only 1.7 and 1.1 μm, respectively), increased resistivity of the surface layer due to a high dislocation density and surface discontinuities due to cavity construction.

The quartz sample tubes were supplied by VirtoCom Ltd., and have inner and outer diameters of 2.0 and 2.4 mm, respectively. An empty tube was found to reduce the resonant frequencies of the TM_{010} and TM_{020} modes by 2.2 and 11.9 MHz, respectively, with negligible reduction in Q factors. This makes them excellent for sensitive measurements of the dielectric properties of powders using the cavity perturbation technique. We have measured the complex permittivity of quartz at 25 °C using these tubes in the same cavity, giving $\varepsilon = 3.80 - j\,0.0003$ at 2.5 GHz, i.e., a loss tangent of less than 10^{-4}.

The sample tubes were filled to a depth of 5 cm with the powder samples (4 cm of which will be in the active region of the cavity), and all samples were left to settle overnight before being measured. The active sample volume is therefore 0.126 cm³. The measured resonant traces showing $|S_{21}|^2$ as a function of frequency are shown in Fig. 3. Only data for the TM_{010} mode are shown here, but the TM_{020} mode exhibits the same qualitative behaviour and data are recorded for both modes.
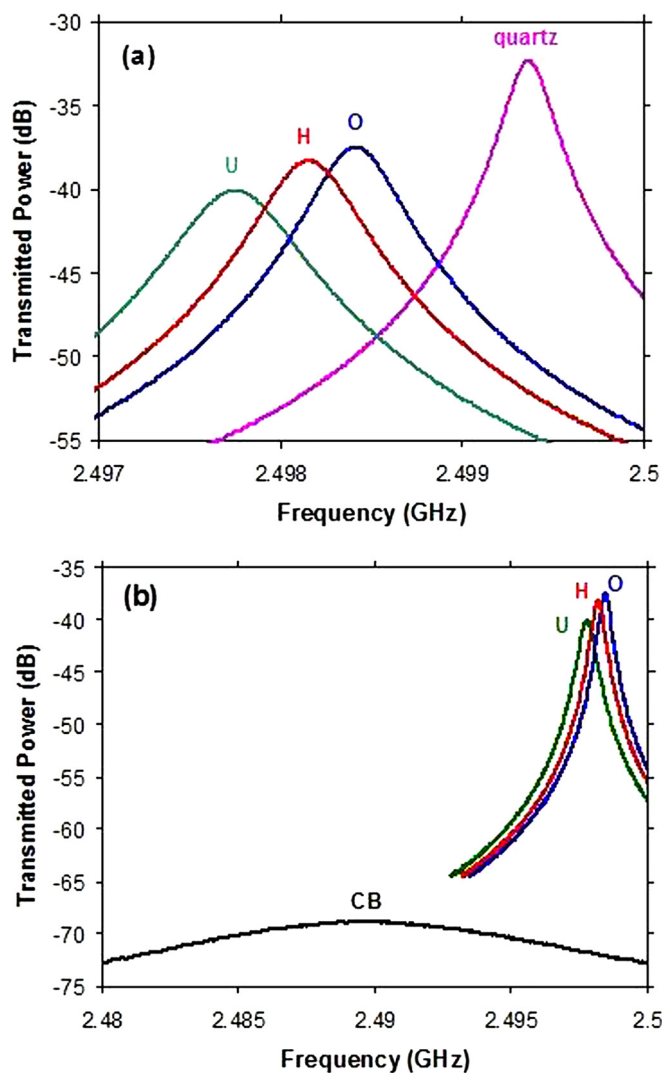
FIG. 3. Resonant traces showing the transmitted power $|S_{21}|^2$ as a function of frequency for the TM_{010} mode. Power samples are contained in thin-walled quartz tubes and the changes in resonant frequency and 3 dB band-widths are measured relative to the empty tubes. (a) The response of an empty quartz tube, together with quartz tubes filled with three nanodiamond samples: one untreated (U), one oxygenated (O), and another hydrogenated (H). (b) The responses of the same three nanodiamond samples, this time compared with the same volume of CB.

To analyse this data, we first define the complex relative permittivity of a dielectric material as $\varepsilon = \varepsilon_1 - j\varepsilon_2$, where ε_1 (or, more properly, $\varepsilon_1 - 1$) quantifies the polarisation of the dielectric material in an applied electric field, whilst ε_2 quantifies the dielectric loss. We use first order cavity perturbation theory to relate the changes in the resonator parameters to the dielectric properties of a sample inserted into the electric field antinode of the cavity.[13] We first define f_0 as the resonant frequency (for either mode) and $f_B = f_0/Q$ as the unloaded 3 dB (or half-power) bandwidth. If a sample is found to reduce the resonant frequency by an amount Δf_0 and increase the 3 dB bandwidth by Δf_B, these are related to the complex permittivity of the sample by the approximate formulae

$$\frac{\Delta f_0}{f_0} \approx (\varepsilon_1 - 1)\frac{V_s}{2V_{eff}}, \tag{1}$$

$$\frac{\Delta f_B}{f_0} = \Delta\left(\frac{1}{Q}\right) \approx \varepsilon_2 \frac{V_s}{V_{eff}}, \tag{2}$$

where f_0 is the unperturbed resonant frequency, V_s is the sample volume, and V_{eff} is the effective volume of the electric field energy within the cavity. The latter quantity is defined by the volume integral

$$V_{eff} = \int\limits_V \frac{E^2}{E_0^2}\,dV, \tag{3}$$

where E_0 is the electric field at the position of the sample. Evaluating Eq. (3) from the theoretical electric field distributions gives $V_{eff} = \pi a^2 L\, J_1^2(p_{0n})$ for the TM_{0n0} modes, i.e., effective volumes of 71.7 cm^3 and 30.8 cm^3 for the TM_{010} and TM_{020} modes, respectively.

Alternatively, the effective volume can be determined experimentally by the calibration measurement of a known material of known geometry. We use stainless steel spheres, since a metal sphere will develop a known electric dipole moment $p = 4\pi\varepsilon_0 b^3 E_0$ (where b is the sphere radius) and then Eq. (1) reduces to $\Delta f_0/f_0 \approx 2\pi b^3/V_{eff}$. We measure the frequency shifts of seven sizes of individual spheres with radii b in equal steps from 0.5 mm to 3.5 mm, each positioned centrally in the cavity, then we use linear regression to evaluate V_{eff} for each mode. This experimental process yields $V_{eff} = 68.3 \pm 0.7$ cm^3 and 28.9 ± 0.3 cm^3 for the TM_{010} and TM_{020} modes, respectively. These are a few % smaller than the calculated values owing to the slight reduction of the electric field in the vicinity of the axial sample holes, and the small distortion of field around the coupling probes (since introducing any non-uniformity in the electric field results in a reduction of V_{eff}, as can be seen directly from Eq. (3)). We use these experimental values for V_{eff} in all of our calculations based on Eqs. (1) and (2).

The experimental cavity perturbations Δf_0 and Δf_B and the calculated values of complex permittivity for the three nanodiamond samples (U, O, and H) sample are shown in Table I (for the TM_{010} mode at 2.5 GHz) and Table II (for the TM_{020} mode at 5.73 GHz), together with the CB powder for comparison. These perturbations are measured relative to the same empty quartz tube in each case. We find that the volumes of the tubes vary by approximately $\pm1\%$, which accounts for the largest systematic error in the calculation of permittivity. Here, we quote values for the effective permittivity $\varepsilon_{eff} = \varepsilon_{1,eff} - j\varepsilon_{2,eff}$ of the powders, since most of the space within the sample tube is air and an effective medium approach is needed to extract the intrinsic permittivity ε of

TABLE I. Change in resonant frequency and 3 dB bandwidth (relative to an empty quartz tube) on introducing the each sample into the TM_{010} mode at 2.5 GHz. Also shown are the resulting (effective) values of the complex permittivity. The random errors in these two experimental parameters (assessed by repeated measurement) are small, around $\pm1\%$. Variation in the volumes of the quartz tubes introduces an additional systematic error of approximately $\pm1\%$, resulting in an overall error of approximately $\pm1.4\%$ in the calculated values of permittivity.

Sample	Δf_0 (MHz)	Δf_B (MHz)	$\varepsilon_{1,eff} - 1$	$\varepsilon_{2,eff}$
Untreated (U)	1.73 ± 0.02	0.353 ± 0.004	0.75 ± 0.01	0.077 ± 0.002
Oxygenated (O)	1.08 ± 0.01	0.204 ± 0.002	0.47 ± 0.01	0.044 ± 0.001
Hydrogenated (H)	1.32 ± 0.01	0.246 ± 0.002	0.57 ± 0.01	0.053 ± 0.001
CB	9.8 ± 0.1	17.0 ± 0.2	4.27 ± 0.06	3.69 ± 0.05

TABLE II. Change in resonant frequency and 3 dB bandwidth (relative to an empty quartz tube) on introducing the sample into the TM_{020} mode at 5.73 GHz, with resulting (effective) values of complex permittivity. Errors are the same % values as for Table I.

Sample	Δf_0 (MHz)	Δf_B (MHz)	$\varepsilon_{1,eff} - 1$	$\varepsilon_{2,eff}$
Untreated (U)	8.88 ± 0.09	2.19 ± 0.02	0.71 ± 0.01	0.088 ± 0.002
Oxygenated (O)	5.55 ± 0.06	1.00 ± 0.01	0.45 ± 0.01	0.040 ± 0.001
Hydrogenated (H)	6.78 ± 0.07	1.30 ± 0.01	0.55 ± 0.01	0.052 ± 0.001
CB	70.3 ± 0.7	103 ± 1	5.64 ± 0.07	4.15 ± 0.06

the actual powder grains. The untreated sample (U) has the largest polarisation $\varepsilon_{1,eff} - 1$ and loss $\varepsilon_{2,eff}$ of the three nanodiamond samples. Oxygenation of the original sample (O) causes these to reduce, and subsequent hydrogenation (H) leads to a partial return to the untreated state.

As can be seen from the results for the CB sample, a high degree of sp^2 hybridisation causes large values of both microwave polarisation $\varepsilon_{1,eff} - 1$ and loss $\varepsilon_{2,eff}$. Using this as a benchmark, we conclude that the greatest degree of sp^2 hybridisation is found in the untreated sample (U), as we might have expected. Annealing in oxygen (O) removes the most sp^2 bonding, followed by hydrogen annealing (H).

In order to quantify our analysis, and so relate the microwave results to the physical structure of the nanoparticles, we have developed a simple, quasistatic model. In this, we assume that each nanoparticle is spherical, with a single crystal diamond core (i.e., which is fully sp^3 hybridised), each with an outer shell which is fully sp^2 hybridised. We then apply the Maxwell-Garnett effective medium model[14] to develop the effective permittivity ε_{eff} of a macroscopic powder composed of close-packed, layered nanoparticles. This is the effective permittivity that has been measured and is presented in Tables I and II.

For the relative permittivity of the sp^2 shell layer in the range $|\varepsilon_s| < 100$, our model shows that the values of $\varepsilon_{2,eff}$ in Tables I and II are directly proportional (to a systematic error of less than 5%) to the volume fractions of sp^2 hybridised material as one would expect. Here, we assume that the diamond core has a negligible microwave loss in comparison with the outer shell layer. Hence, from the combined results of Tables I and II, we deduce that the O sample has the smallest volume of sp^2 hybridised carbon, the H sample has $(53/42) - 1 = 26\%$ more, whilst the U sample has $(83/42) - 1 = 98\%$ more. Such values can be deduced directly from the changes in resonant bandwidth and so are subject to experimental errors of less than $\pm 3\%$, which emphasises the power and convenience of this microwave absorption technique for such nanodiamond characterisation. Absolute values of the volume fractions are subject to large uncertainties owing to the experimental uncertainty in extracting representative

values of ε_s from the carbon black data. Also, layer thicknesses may not be meaningful, since the sp^2 layer itself may not be continuous. However, the ability to study such small variations in the volume of surface bound sp^2 carbon present is of great benefit.

We have a high degree of confidence in using these microwave measurements to characterise the degree of sp^2 hybridisation in nanodiamond samples and find that the trends are highly reproducible. There is only a slight frequency dependence in the properties between 2.5 GHz and 5.7 GHz, so in practice either cavity modes can be used for these measurements.

Very few other techniques are able to study such small variations in surface bound sp^2 with a comparable degree of sensitivity and simplicity. The Raman spectra of Fig. 1 demonstrate the difficulty in measuring such small changes and are also vulnerable to heating effects and damage of the particles by the laser irradiation (particularly visible Raman). This approach is highly reproducible, simple, and can be quantitative with further investigations and model development.

[1] O. A. Williams, O. Douheret, K. Daenen, K. Haenen, E. Osawa, and M. Takahashi, Chem. Phys. Lett. **445**(4-6), 255–258 (2007).
[2] J. I. Chao, E. Perevedentseva, P. H. Chung, K. K. Liu, C. Y. Cheng, C. C. Chang, and C. L. Cheng, Biophys. J. **93**(6), 2199–2208 (2007).
[3] R. Lam and D. Ho, Expert Opin. Drug Delivery **6**(9), 883–895 (2009).
[4] V. N. Mochalin, O. Shenderova, D. Ho, and Y. Gogotsi, Nat. Nanotechnol. **7**(1), 11–23 (2012).
[5] A. Chaudhary, J. O. Welch, and R. B. Jackman, Appl. Phys. Lett. **96**(24), 242903 (2010).
[6] S. A. Maksimenko, V. N. Rodionova, G. Y. Slepyan, V. A. Karpovich, O. Shenderova, J. Walsh, V. L. Kuznetsov, I. N. Mazov, S. I. Moseenkov, A. V. Okotrub, and P. Lambin, Diamond Relat. Mater. **16**(4–7), 1231–1235 (2007).
[7] S. Osswald, G. Yushin, V. Mochalin, S. O. Kucheyev, and Y. Gogotsi, J. Am. Chem. Soc. **128**(35), 11635–11642 (2006).
[8] J. Hees, A. Kriele, and O. A. Williams, Chem. Phys. Lett. **509**, 12 (2011).
[9] O. A. Williams, J. Hees, C. Dieker, W. Jager, L. Kirste, and C. E. Nebel, ACS Nano **4**(8), 4824–4830 (2010).
[10] S. Ghodbane, A. Deneuville, D. Tromson, P. Bergonzo, E. Bustarret, and D. Ballutaud, Phys. Status Solidi A **203**(10), 2397–2402 (2006).
[11] A. C. Ferrari and J. Robertson, Phys. Rev. B **63**(12), 121405 (2001).
[12] A. C. Metaxas and R. J. Meredith, *Industrial Microwave Heating* (P. Peregrinus on behalf of the Institution of Electrical Engineers, London, UK, 1983).
[13] O. Klein, S. Donovan, M. Dressel, and G. Gruner, Int. J. Infrared Millim. Waves **14**(12), 2423–2457 (1993).
[14] T. C. Choy, *Effective Medium Theory: Principles and Applications, International Series of Monographs on Physics* (Oxford University Press, Oxford, UK, 1999).